EVS24
Stavanger, Norway, May 13-16, 2009

The Hierarchy Control System of Intelligent Hybrid Electric Vehicle

Yugong Luo, Tao Chen, Guoqiang Zhou, Keqiang Li
State Key Laboratory of Automotive Safety and Energy, Tsinghua University, Beijing, 100084
email: lyg@mail.tsinghua.edu.cn

Abstract

In this paper, coordinating vehicle safety, energy conservation and environmental protection, an Intelligent Hybrid Electric Vehicle (IHEV) which is integrated with advanced technologies of intelligent vehicle and new energy vehicle has been designed. A new hierarchical control structure is proposed and applied into the vehicle control system, and then the vehicle control strategy is evaluated and verified by simulated and experimental analysis. After a brief introduction of IHEV, a particular procedure of the hierarchical control strategy is presented, which includes intelligent driving assistance control object determination layer, total driving/braking torque determination layer, total torque distribution layer and torque coordinate control layer. Many simulations and experiments are carried out by the forward simulation platform and the prototype test vehicle. The simulation and experiment results show, by applying the hierarchy control system to the IHEV, the IHEV can successfully and smoothly realize all of the functions while guarantee the optimal safety, economical performance and driving comfort.

Keywords: hybrid electric vehicle, intelligent vehicle, hierarchical control system, active safety

1 Introduction

These days, great efforts have been paid by the Automobile Industry to pursue vehicles that are safer, more fuel efficient and more environmental friendly. Two trends are making significant progress, separately. Towards the vision of accident-free driving, active safety technologies, such as Adaptive Cruise Control, have been widely developed. Towards the trend of more fuel efficient and more environmental friendly vehicle, low fuel consumption driving systems, e.g. hybrid electric driving systems, have been well developed and put into the market. As the most promising new energy vehicle, the hybrid electric vehicle (HEV) has been extensively researched and applied, from the 1997 Toyota's Prius, there are more than 2 million HEVs sold out[1]. As the key technology of HEV, the power management strategy is focused, which includes various engineering control strategies [2][3] and various applications by classical and modern control theory [4][5][6][7].
As the most advanced active safety technology, the Intelligent Vehicle (IV) technology has also been widely and deeply researched from 70s last century, excellent fruition has been achieved on driving assistance warning system [8][9], driving assistance control system [10][11] and automatic driving system [12][13].
One promising trend, would integrate these two separate trends together, which would be Intelligent Hybrid Electric Vehicle（IHEV）. Not only can the IHEV provide the benefits of enhanced active safety, better driving comfort and more fun of driving, but also can this system reach the combined advantages of low fuel consumption, low emission and what's more, low noise. In this

field, although Toyota Company has introduced a hybrid electric vehicle LS600hl with intelligent driver assistance function [14], the relevant technology has never been reported. Professor Masao Nagai has carried out the pure electric vehicle control research with intelligent driver assistance function [15].

In the author's research group, a joint study in this area with China FAW Corporation and Chang'an Automobile Corporation is promoting since 2006, aiming to develop a new conceptual vehicle, which combined hybrid propulsion system, electronically controlled chassis, quipped with advanced sensors and in-vehicle network. After 3 years' joint development, the Besturn Intelligent Hybrid Electric Vehicle is successfully developed. This paper will present a hierarchical control system of the IHEV, and the vehicle performance will be verified and evaluated by several simulations and experiments with the forward simulation platform and prototype test vehicle.

2 Intelligent Hybrid Electric Vehicle configuration

The proposed IHEV configuration is shown in Fig. 1.

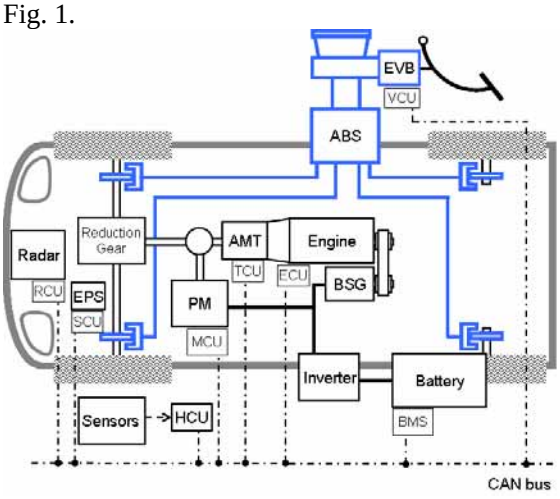

Fig. 1 Configuration of IHEV

The IHEV is composed of traffic environment and vehicle states sensing sub-system, hybrid electric propulsion sub-system, driving assistance sub-system, control sub-system and communication network sub-system. The traffic environment and vehicle states sensing sub-system mainly includes Millimeter-wave radar sensor, driving assistance function switch, set speed switch, longitudinal acceleration sensor, accelerator pedal position sensor, brake pedal position sensor, transmission position sensor and ignition switch position sensor. The hybrid electric propulsion sub-system mainly includes a 1.5-liter gasoline engine, 20KW driving motor, 5KW generator (BSG), 6Ah power battery and 5 speed automatic transmission. The driving assistance sub-system mainly includes hydraulic brake assembly equipped with electric vacuum booster (EVB) and electric power steering (EPS) assembly. The control sub-system mainly includes hybrid vehicle control unit (HCU), radar control unit (RCU), engine control unit (ECU), transmission control unit (TCU), motor control unit (MCU), battery management system (BMS), EVB control unit (VCU) and EPS control unit (SCU). The communication network sub-system mainly includes two high-speed CAN networks, namely power system CAN networks and driving assistance system CAN network, hybrid vehicle control unit performs the CAN gateway function, and the IHEV CAN network topology map is as shown in Fig. 2.

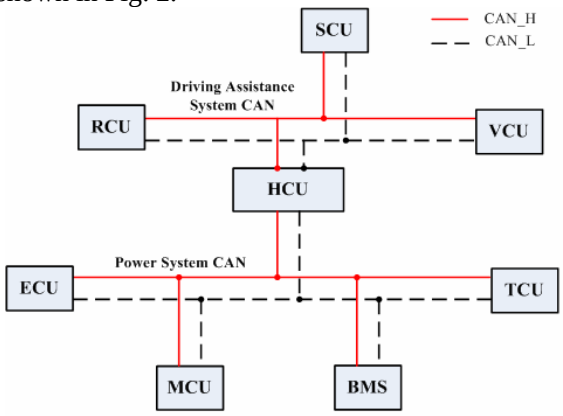

Fig. 2 IHEV CAN network topology map

The intelligent driving assistance mode and manual driving mode are both achieved in IHEV, and along with the various driving situation, it could automatically shift from intelligent driving assistance mode to manual driving mode.

3 Hierarchical Control System Design

The IHEV hierarchical control system is shown in Fig. 3.

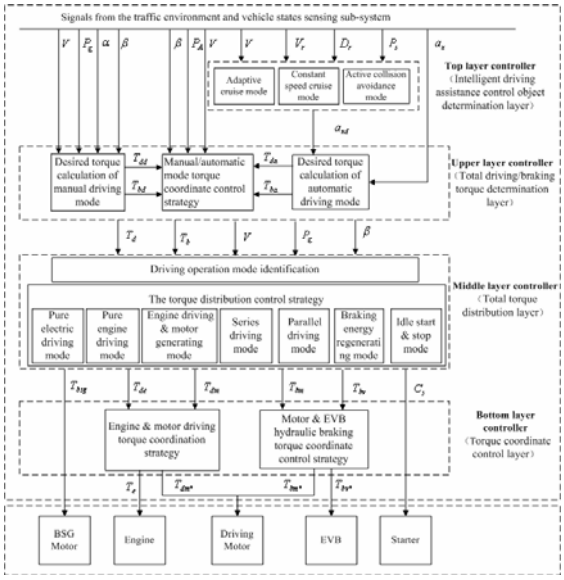

Fig.3. IHEV hierarchical control system scheme

Here, α , β , P_g , P_A , P_s are the accelerator pedal position, brake pedal position, transmission shift position, intelligent driver assistance function switch signal and cruise set switch signal with respect to the driver command, V , V_r , D_r a_x , a_{xd} are ego velocity, relative velocity, relative distance, ego acceleration and desired ego acceleration, respectively; T_{dd} , T_{bd} , T_{da} , T_{ba} , T_d , T_b , T_{de} , T_{dm} , T_{bm} , T_{bh} , T_{bsg} are manual-mode desired driving torque, manual-mode desired braking torque, auto-mode desired driving torque, auto-mode desired braking torque, desired total driving torque, desired total braking torque, desired engine torque, desired motor driving torque, desired motor braking torque, desired hydraulic braking torque, desired BSG torque with respect to the desired torque of the whole system, T_e , T_{dm*} , T_{bm*} , T_{bv*} , C_s are actual engine torque, actual motor driving torque, actual motor braking torque, actual EVB braking torque and the start command of starter.

Four layers compose the IHEV hierarchical control system. The top layer is intelligent driving assistance object determination layer, in which, by synthesizing the ego and preceding vehicle states and the driver-set cruise speed, the intelligent assistance driving sub-mode and desired longitudinal acceleration is decided. The upper layer is total driving/braking torque determination layer, in which, after calculating the manual and automatic desired driving torque, the desired driving and braking torque by considering the driver command and cooperating the different desired torque is formulated. The middle layer is total torque distribution layer, in which, the torque distribution for different components according to the total desired torque and vehicle states is optimized. The bottom layer is torque coordinate control layer, in which, the engine torque, motor torque, and EVB brake torque command are finally determined by applying engine & motor driving torque coordinate control strategy and motor & EVB braking torque coordinate control strategy.

3.1 Intelligent driving assistance control object determination layer

The intelligent driving assistance mode consists of constant speed cruise control sub-mode, adaptive cruise control sub-mode and active collision avoidance control sub-mode. The constant speed cruise control refers to driving at driver set velocity automatically. The adaptive cruise control means following the preceding car within the various velocities while maintaining safety distance. The active collision avoidance control indicates the emergent braking while potential front collision is detected. All sub-modes switching logic are shown in Fig. 4.

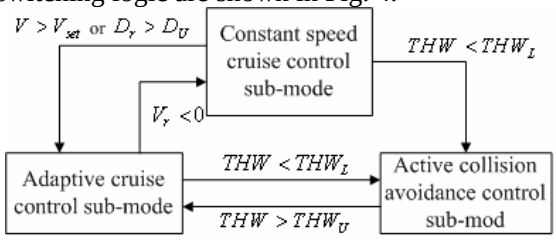

Fig. 4 Intelligent assistance driving sub-modes switching logic

In the Fig. 4, THW is time headway, it is given by

$$THW = D_r / V \quad (1)$$

Where THW_L is the lower limit of time headway, while THW_U , D_U are the upper time headway limit and upper relative distance limit, V_{set} is the driver-set cruise speed.

3.1.1 Constant speed cruise control sub-mode

The desired acceleration of constant speed cruise control sub-mode is

$$a_{xd} = C_{cp}(V_{set} - V) + C_{ci}\int (V_{set} - V)dt \quad (2)$$

Where C_{cp} , C_{ci} could be adjusted with time. The desired acceleration is processed as the equation 3 to avoid excessive acceleration for driving comfort consideration.

$$a_{xd} = \begin{cases} 0.5, & a_{xd} > 0.5 \\ a_{xd}, & -2.5 < a_{xd} < 0.5 \\ -2.5, & a_{xd} < -2.5 \end{cases} \quad (3)$$

3.1.2 Adaptive cruise control sub-mode

The desired acceleration of cruise control sub-mode is given by

$$a_{xd} = C_{a1}(D_r - THW_{dd}V - C_{a2}) + C_{a3}V_r \quad (4)$$

Where, THW_d is cruise time headway based on the driving characteristic, C_{a1}, C_{a2}, C_{a3} are adjustable with time. Also, for driving comfort, the desired acceleration is saturated as equation (3).

3.1.3 Active collision avoidance control sub-mode

The desired acceleration of cruise control sub-mode is as follows

$$a_{xd} = -0.5C_{b1}\frac{V_r^2}{(D_r - THW_{db}V - C_{b2})} \quad (5)$$

Where, THW_{db} is collision avoidance time headway based on the driving characteristic, C_{b1}, C_{b2} are various with time.

3.2 Total driving/braking torque determination layer

In this control layer, the manual/automatic mode's desired torque calculation, manual/automatic mode switching strategy, and driving/braking torque coordination are achieved.

3.2.1 Desired torque calculation of manual driving mode [16]

In the manual driving mode, the "9-point-definition method" which formulates the driving torque demand map is presented for the desired driving torque T_{dd} calculation, shown in Fig. 5. As the parallel regenerative braking system is adopted by the IHEV, the desired braking torque T_{db} is calculated by the definition curve shown in Fig. 6.

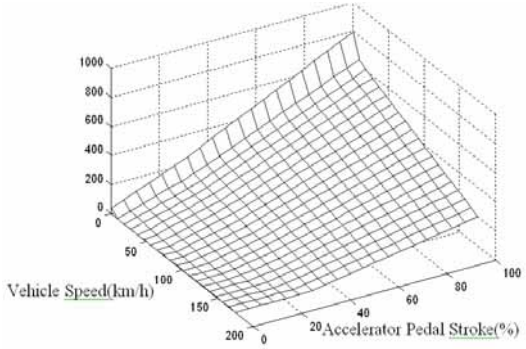

Fig. 5 Desired driving torque definition surface

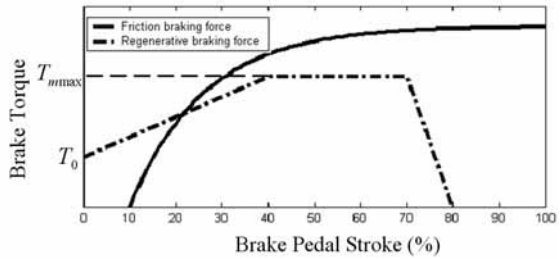

Fig. 6 Desired braking torque definition curve

3.2.2 Desired torque calculation of automatic driving mode

In the automatic driving mode, the desired driving/braking torque is obtained by the following logic shown in Fig. 7.

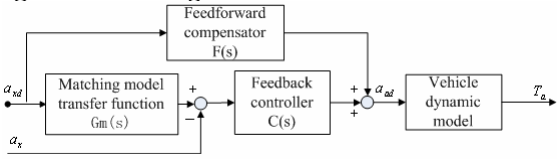

Fig. 7 Desired torque calculation logic in automatic driving mode

Where, the matching model transfer function $G_M(s)$ is given by

$$G_M(s) = \frac{1}{s + 0.5} \quad (6)$$

The feedforward compensator $F(s)$ is

$$F(s) = \frac{G_M(s)}{P(s)} \quad (7)$$

$P(s)$ is the vehicle plant transfer function obtained by system identification.

The Feedback controller $C(s)$ is

$$C(s) = C_p(a_{xd} - a_x) + C_i\int(a_{xd} - a_x)dt \quad (8)$$

Where, C_P, C_i are adjustable parameters.

The driving/braking torque is determined by the following vehicle dynamic equation

$$T_a = \frac{r}{\eta i_g i_d}(Ma_{ad} + Mgf + C_d A V^2) \quad (9)$$

Where, M , g , f are vehicle mass, acceleration of gravity and rolling resistance coefficient, C_d , A , r , i_g , i_d , η are air resistance coefficient, equivalent front face area, wheel radius, transmission gear ratio, final drive gear ratio and mechanical transmission efficiency.

3.2.3 Manual/automatic mode switching strategy

The manual/automatic driving mode switching strategy is as follows

$$\text{mod}=\begin{cases}0, & \alpha>0 \ or \ \beta>0 \ or \ V<V_{\min}\\ 1, & \alpha=0,\beta=0,P_A=1,V>V_{\min}\end{cases} \quad (10)$$

Where, mod is the output driving mode, 0 refers to manual driving mode, while 1 refers to automatic driving mode, $P_A=1$ stands for intelligent assistance driving function enable, $V_{\min}$ is the minimal velocity in automatic driving mode.

3.2.4 Driving/braking torque coordinate control strategy

During the manual/automatic driving mode dynamic switching process, there could be a torque mutation due to the independent desire torque calculation of each driving mode. If not effectively controlled, the impact of torque mutation would result in not only driving discomfort, but also lower transmission system life. So the various reference driving/braking torque curve during the dynamic switching process is presented, which is as follows

$$T_{t_n}(k+1)=\frac{T_{t_0}(k)-T_{t_n}(k)}{t_n-k\delta}\delta+T_{t_n}(k) \quad (11)$$

Where, t_n , δ are the total switching time of dynamic process and sample time, $T_{t_n}(k)$, $T_{t_0}(k)$, $T_{t_n}(0)$ are the desired output driving torque in the switching process, objective driving mode desired driving torque and original driving mode desired driving torque.

3.3 Total torque distribution layer

The control strategy in third layer is composed of operation mode identification and torque distribution strategy. Identifying the operation mode is one of the key points to the third layer on the basis of current vehicle states (velocity, actual gear, SOC, etc.) and the total torque demand from the second layer. The vehicle driving operation mode is given by the Fig. 8.

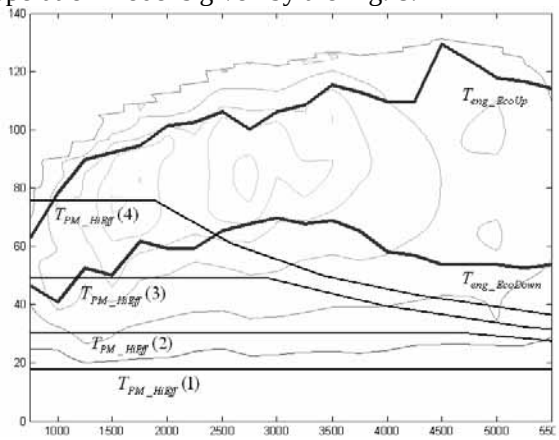

Fig. 8 Driving operation mode identification

As shown in Fig. 8, when the desired driving torque is between curve T_{eng_EcoUp} and $T_{eng\_EcoDown}$, the operation mode is engine driving mode. While above the curve T_{eng_EcoUp} , the operation mode is parallel driving mode. Below the curves $T_{PM\_HiEff}(N)$, N = 1, 2, 3, 4, 5, the pure electric driving mode and series driving mode are obtained (based on the SOC). When the desired driving torque is between the curve $T_{PM\_HiEff}(N)$ and $T_{eng\_EcoDown}$, the operation mode is engine driving& motor generating mode. In Fig. 8, $T_{PM\_HiEff}(N)$ is the high-efficiency working curve in gear N which has been already converted into engine side.

When $\beta>\beta_{low}$ *or* $T_b>T_{blow}$, the braking energy regenerating mode is activated, while in the idle start & stop mode, engine fuel is cut off on condition that $V=0, T_d=0$ and start up when necessary.

The torque distribution formulation in pure electric driving mode is as follows

$$\begin{cases}T_{de}=0\\ T_{dm}=T_d\\ T_{bsg}=0\end{cases} \quad (12)$$

While in series driving mode, the equation is performed as

$$\begin{cases}T_{de}=2W_{soc}T_{bsg\_rete}\\ T_{dm}=T_d\\ T_{bsg}=W_{soc}T_{bsg\_rete}\end{cases} \quad (13)$$

Where the T_{bsg_rate} , W_{SOC} are BSG nominal generating torque and charge coefficient based on SOC.

The torque distribution formulation in pure engine driving mode is

$$\begin{cases} T_{de} = T_d \\ T_{dm} = 0 \\ T_{bsg} = 0 \end{cases} \quad (14)$$

At the same time in the engine driving & motor generating mode, it is given by

$$\begin{cases} T_{de} = T_{e\_ecodown} \\ T_{dm} = 0 \\ T_{bsg} = -W_{soc} \min(T_{bsg\_rate}, (T_{e\_ecodown} - T_d / 2)) \end{cases} \quad (15)$$

Where, $T_{e\_ecodown}$ is the lower limit torque curve of engine economical working area.

The torque distribution strategy in parallel driving mode is given by

$$\begin{cases} T_{de} = \min(T_{e\_\max}, T_d - T_{dm*} / 2) \\ T_{dm} = \min(T_{m\_\max}, (T_d - T_{e\_ecoup}) i_g) \\ T_{bsg} = 0 \end{cases} \quad (16)$$

Where, T_{e_ecoup} , $T_{e\_\max}$, $T_{m\_\max}$ are the upper limit torque of engine economical working area, maximum engine torque and maximum motor driving torque.

The torque distribution strategy in braking energy regenerating mode is given by

$$T_{bm} = \begin{cases} \min(C_e * T_{e\_\max}, T_b), & \beta = 0 \\ \min(T_{e\_\max}, T_b), & \beta \neq 0 \end{cases}$$

$$T_{bv} = \begin{cases} T_b - T_{bm}, & \beta = 0 \\ 0, & \beta \neq 0 \end{cases} \quad (17)$$

Where, C_e is the adjustable parameter.

The torque distribution strategy in idle start & stop mode is given by

$$T_{bsg} = \begin{cases} T_{start}, & SOC > SOC_{low} \\ 0, & SOC \le SOC_{low} \end{cases}$$

$$C_S = \begin{cases} 0, & SOC > SOC_{low} \\ 1, & SOC \le SOC_{low} \end{cases} \quad (18)$$

Where, SOC_{low} is the lower SOC limit of battery, and the traditional starter starts the engine when C_s equals to 1.

3.4 Torque coordinate control layer

The bottom layer strategy is mainly comprised of the engine & motor driving torque coordinate control strategy and motor & EVB hydraulic braking torque coordinate control strategy.

3.4.1 Engine & motor driving torque coordination strategy

When the driving sub-mode switches between the engine driving mode and pure electric motor driving mode, although the target driving torques equals during the switching process, there is great different responsible character between the engine and motor, which will lead to driving discomfort and lower power system life. The driving torque coordinate control strategy is presented during the dynamic switching process as follows

$$\begin{cases} T_e(k+1) = \dfrac{T_{de}(k) - T_{e\_act}(k)}{t_n - k\delta} \delta + T_e(k) \\ T_{dm*}(k+1) = \dfrac{T_{dm}(k) - T_{de}(k) + T_{e\_act}(k)}{t_n - k\delta} \delta + T_{dm*}(k) \end{cases} \quad (19)$$

Where, t_n , δ are the total switching time of dynamic process and sample time, $T_{de}(k)$, $T_e(k)$, $T_{e\_act}(k)$, $T_{dm}(k)$, $T_{dm*}(k)$ are the desired engine torque of target mode, desired output engine torque during the dynamic switching process, actual engine torque, desired motor torque of target mode and desired output motor torque during the dynamic switching process.

3.4.2 Motor & EVB hydraulic braking torque coordinate control strategy

According to the third layer strategy, EVB is activated since the braking torque exceeds the motor braking torque limit. Compared with the motor torque response, the EVB hydraulic braking torque has not only slow response but also poor accuracy. Therefore, if there is no coordinated control on the motor & EVB braking torque, the actual total braking torque response will be very slow and inaccurate especially in the emergency braking situation. The dynamic coordinate control is investigated, which is as follows

$$\begin{cases} T_{bv*}(k+1) = \dfrac{T_{bv}(k) - T_{bv\_act}(k)}{t_n - k\delta} \delta + T_{bv*}(k) \\ T_{bm*}(k+1) = T_{bm*}(k) + T_{bv}(k) + T_{bm}(k) - T_{bv*}(k) \end{cases} \quad (20)$$

Where, t_n, δ are the total time of dynamic process and sample time, $T_{bv}(k)$, $T_{bv*}(k)$, $T_{bv\_act}(k)$, $T_{bv\_act}(k)$, $T_{bm}(k)$, $T_{bm*}(k)$ are the

EVB target braking torque, desired output EVB torque during the dynamic process, actual EVB torque, motor target braking torque and desired output motor torque during the dynamic process.

4 Control strategy simulation analysis and evaluation

After the control strategy development, the IHEV forward simulation platform based on MATLAB/SIMULINK has been established, of which the structure is shown in Fig. 9.

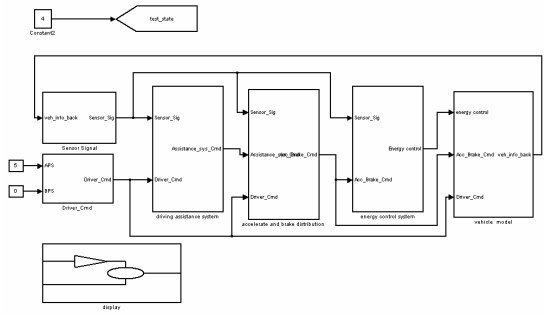

Fig. 9 IHEV forward simulation platform structure

As shown in Fig. 9, the IHEV forward simulation platform is composed of 7 sub-models: simulation observer sub-model, driver command sub-model, sensor signals simulation sub-model, top-level control sub-model, 1st level control sub-model, middle and bottom control sub-model, vehicle components and dynamics sub-model. The constant speed cruise operating mode, adaptive sinusoidal following operating mode and active collision avoidance operating mode are analyzed with IHEV simulation platform in the following sections.

4.1 Constant speed cruise operating mode

The initial cruise speed is set to 60km/h, in the course the cruise speed is adjusted to 68 km/h by driver, and the initial ego velocity is 40km/h, simulation result is shown in Fig. 10.

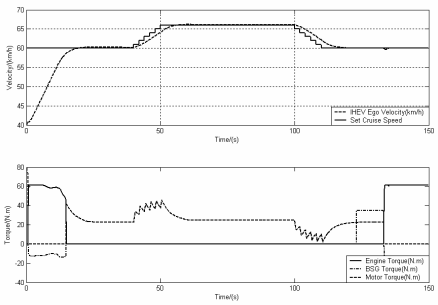

Fig. 10 Constant speed cruise operating mode simulation result

In Fig. 10, the velocity and engine, motor, BSG torque curves are obtained. As shown, after the cruise control enabled, ego vehicle accelerates to the driver set cruise speed in quite a short time, and along the various set-cruise speed, it accurately following speed with less than 5%. During the constant speed cruise process, the IHEV driving mode switches from engine driving & motor generating mode to pure electric driving mode, and then back to engine driving & motor generating mode.

4.2 Adaptive sinusoidal following operating mode

In this operating mode, preceding velocity is assumed to sine wave in 55km/h to 75km/h, the initial ego velocity is 40kn/h, and the simulation result is shown in Fig. 11.

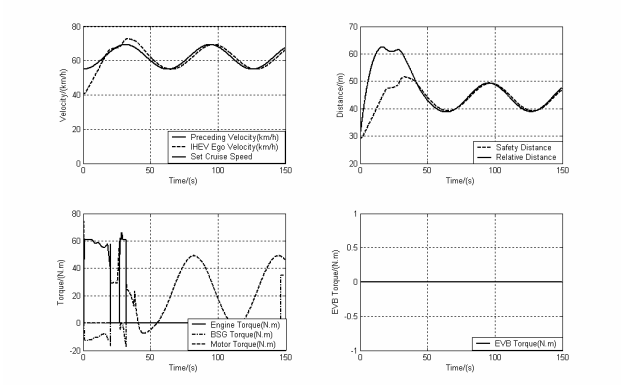

Fig. 11 Adaptive sinusoidal following operating mode simulation result

In Fig. 11, the ego velocity, actual and safety distance, engine, driving motor, BSG motor and EVB braking pressure curves are obtained. Although a little time delay, not only is the following performance very good except for the initial dynamic following process from 40km/h to 60km/h with a short time over acceleration, but also it maintains a comfortable safety distance.

In order to compare IHEV fuel economy with the traditional intelligent vehicle, the adaptive sinusoidal following operating mode is tested. The engine operating points of both IHEV and IV are obtained, which is shown in Fig. 12. Table 1 shows the fuel consumption of each vehicle.

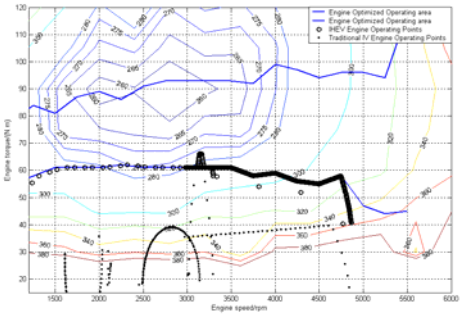

Fig. 12 Engine operating points of IHEV and IV comparison

Table 1: Fuel consumption of 100-kilometres of this mode

vehicle	Fuel consumption
IHEV	3.85L/100km
Traditional Intelligent Vehicle	5.63L/100km

From the simulation results, it shows that the IHEV always keeps in the presetting optimized engine operating range. But with only one power source, the engine operating points of traditional intelligent vehicle is limited by various power demand, ultimately resulted in 46.2% increase in fuel consumption.

4.3 Active collision avoidance operating mode

In this operating mode, ego vehicle moves forward with initial speed of 40km/h, 13 meters in front of which, suddenly appears a static obstructions. Therefore, the system automatically enters the active collision avoidance mode with the biggest braking strength until stop. Also, the IHEV and traditional intelligent vehicle is compared here, which is shown in Fig13.

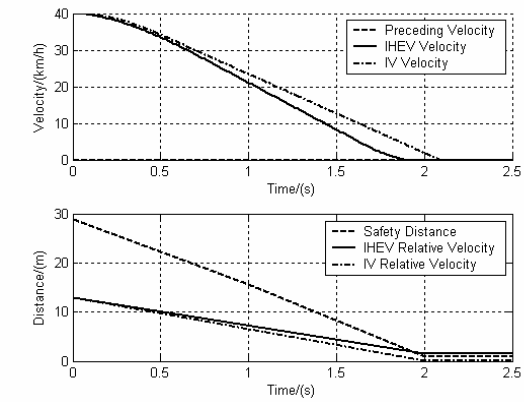

Fig. 13 Active collision avoidance operating mode simulation result of IHEV and IV comparison

Shown in the Fig. 13, the traditional intelligent vehicle with EVB brake has a slower response. Therefore at 1.7s forward collision happens. While, due to the motor's fast response in the early braking, the braking demand can be achieved quickly and accurately, then followed by joint EVB braking, the vehicle can stop faster with about 1m distance to the front static obstructions.

5 Experiment Verification of control strategy

After the control strategy development and simulation analysis, the group has design the Besturn IHEV (as shown in Fig.14), and the RCP is developed based on MICROAUTOBOX, finally experiments are carried out and the control strategy is evaluated.

Fig. 14 Besturn IHEV

The cruise operating mode, Adaptive sinusoidal following operating mode and active collision avoidance operating mode are all tested by Besturn IHEV.

5.1 Cruise operating mode

In this operating mode, the driver set cruise speed is trapezoidal changed. Cruise control mode is enabled in the 49s. The experiment is shown in Fig. 15.

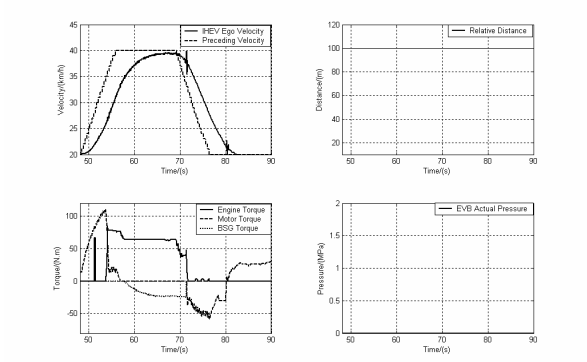

Fig. 15 Cruise operating mode experimental result

As shown in Fig. 15, the set cruise speed increases rapidly from 20km/h, and ego vehicle starts to accelerate in pure electric motor drive mode. With speed accumulated and demand torque increasing, the IHEV is shifted to engine drive mode. When entering a state of uniform traffic, the control system launches into engine drive & motor generation mode. Then the braking energy regeneration mode is obtained as the set speed decreasing, during which motor provides all the

braking power. In the whole process, the system time delay is a little large.

5.2 Adaptive sinusoidal following operating mode

In this operating mode, preceding velocity is sine wave from 20km/h to 35km/h, the initial ego velocity is 17km/h. The experiment result is shown in Fig. 16, 17.

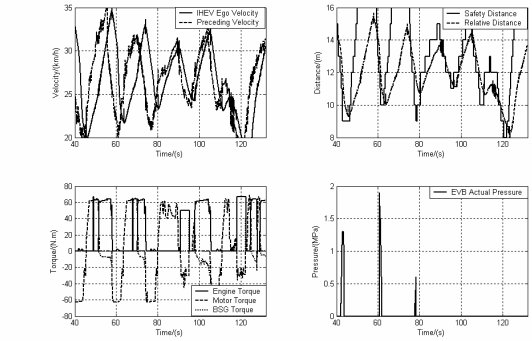

Fig. 16 Adaptive sinusoidal following operating mode experimental result

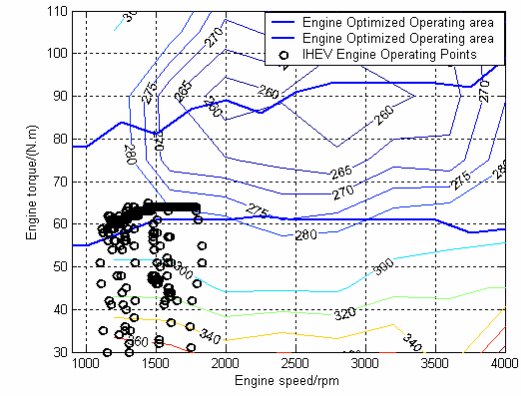

Fig. 17 Engine operating points of IHEV

Results shows, in the initial stage of sinusoidal following as transition phase, the IHEV follows with a slower and larger error. In the first sine cycle, the parallel drive mode is selected due to the large demand acceleration. As error decreases, the torque demand reduces, and engine driving & motor generating mode is achieved. Then with power demand further reduced, IHEV works in the pure electric driving mode. By a sudden slowdown of preceding vehicle, the ego then follow a big deceleration with both motor braking and EVB braking, which maintains a desired relative velocity and safety distance.

Subsequently, since the vehicles enter the stable phase, an excellent sinusoidal following is achieved, during which both velocity and distance errors keep small, and the IHEV driving mode switches seamlessly among pure electric driving, engine driving & motor generating, parallel driving and braking energy regenerating modes.

As shown in Fig. 18, engine operating points with black o are obtained, and most actual engine operating points are within the engine economic range that can effectively improve vehicle fuel economy.

5.3 Active collision avoidance operating mode

In this operating mode, ego vehicle moves forward with initial speed of 30km/h, when 15 meters in front of which appears a static vehicle. Therefore, the active collision avoidance control activated with emergency braking strength until stop which is shown in Fig18.

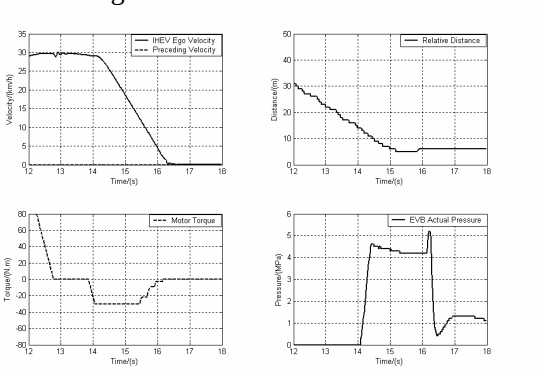

Fig. 18 Active collision avoidance operating mode experimental result

As shown in Fig. 18, since the active collision avoidance control is enabled, the motor brakes with the maximum torque while EVB with 4MPa braking strength. Vehicle speed decreases sharply until stop within 5m to the front vehicle, and then system quits the active collision avoidance control automatically.

6 Conclusions

(1) The established IHEV hierarchical control system can achieve the integrated and coordinated control on multiple subsystems, which guarantees all the driving functions and the optimal safety, economy and driving performance of the vehicle.

(2) Manual and automatic driving modes have been designed in the developed hierarchical control system, and the control strategy is designed to smooth the switch dynamic process in order to keep the IHEV driving comfort.

(3) In the constant speed cruise control mode and adaptive cruise control mode of this hierarchical control system, not only is safety and driving strength performance achieved, but also the

optimized fuel economy is obtained.
(4) In the active collision avoidance control mode of this hierarchical control system, the braking torque responds more accurately and faster, therefore, active safety performance is upgraded.

Acknowledgments

This work was supported by the FAW research center. The authors would like to thank Mr. Liu Minghui and Mr. Liu dongqing for their kindness help in development of the Besturn intelligent hybrid vehicle.

References

[1] http://www.hybridcars.com

[2] Luo Yugong, Yang Diange, Jin Dafeng, Li, Keqiang, Lian Xiaomin. Development of powertrain controller for mild hybrid electric vehicle. Jixie Gongcheng Xuebao/Chinese Journal of Mechanical Engineering, v 42, n 7, p 98-102, July 2006

[3] S. Fiorenza, R. Lanzafame and M. Messina. Analysis of Rules-Based Control Strategies for Integrated Starter Alternator Vehicles. SAE TECHNICAL PAPER 2008-01-1314.

[4] Travis A. Anderson, Joseph M. Barkman, Chris Mi. Design and Optimization of a Fuzzy-Rule Based Hybrid Electric Vehicle Controller. IEEE Vehicle Power and Propulsion Conference (VPPC), September 3-5, 2008, Harbin, China

[5] S. WAHSH, H. G. HAMED, M. N. F. NASHED, T. DAKRORY. Fuzzy Logic Based Control Strategy for Parallel Hybrid Electric Vehicle. Proceedings of 2008 IEEE International Conference on Mechatronics and Automation.

[6] Sylvain Pagerit, Aymeric Rousseau, Phil Sharer. Global Optimization to Real Time Control of HEV Power Flow example of a Fuel Cell Hybrid Vehicle. EVS21, 2004

[7] Cleber Willian Gomes, Adriane Paulieli Colossetti, et al. Computational Methods for Management of Hybrid Vehicles. SAE TECHNICAL PAPER 2008-36-0262

[8] Said Mammar, Sebastien Glaser, Mariana Netto, "Time to Line Crossing for Lane Departure Avoidance: A Theoretical Study and an Experimental Setting", IEEE Transactions of Intelligent Transportation Systems, VOL. 7, NO. 2, June 2006

[9] Nakaoka, M., Raksincharoensak, P., Nagai,M., "Study on Forward Collision Warning System Adapted to Driver Characteristics and Road Environment", Control, Automation and Systems, 2008. ICCAS 2008. International Conference on 14-17 Oct. 2008 Page(s):2890 - 2895

[10] Hellstrom E, Ivarsson M, et al. Look-ahead control for heavy trucks to minimize trip time and fuel consumption. Control Engineering Practice, 17(2), 2008: 245-254

[11] Yamamura Y, Seto Y, et al. An ACC design method for achieving both string stability and ride comfort. Journal of System Design and Dynamics, 2008, 2(4): 979-990.

[12] Lotfi Beji, Yasmina Bestaoui. An adaptive control method of automated vehicles with integrated longitudinal and lateral dynamics in road following. Second workshop on Robot Motion and Control, 2001: 201-206.

[13] Michael Darms, Paul E. Rybski, Chris Urmson. A multisensor multiobject tracking system for an autonomous vehicle driving in a urban environment. AVEC'08 Kobe, Japan, Oct. 6-9, 2008

[14] http://www.lexus.com.cn

[15] MASAO NAGAI. Vehicle motion control issues using micro electric vehicle 'NOVEL'. EVS-22 Yokohama, Japan, Oct. 23-28, 2006

[16] Zhou, Lei; Luo, Yugong; Yang, Diange; Li, Keqiang; Lian, Xiaomin. Development of hybrid powertrain control system for parallel-series hybrid electric vehicle. Jixie Gongcheng Xuebao/Chinese Journal of Mechanical Engineering, v 43, n 4, p 125-131, April 2007

Author

Dr. Yugong Luo works at department of automotive engineering of Tsinghua University as an associate professor. The research interests include the vehicle dynamics control of HEV&PEV, the global chassis control and the intelligent vehicle control. Until now, Dr. Luo has published more than 40 papers and gotten 9 patents of invention